Structure and properties of some new dihydropyrazine–tetracyanoquinodimethane charge transfer salts

David J. R. Brook† and Tad H. Koch*

Department of Chemistry and Biochemistry, University of Colorado, Boulder, Colorado 80309-0215, USA

Rapid crystallization of acetonitrile solutions containing 4a,8a-diaza-2,6-dioxa-3,4,7,8-tetrahydro-4,4,8,8-tetramethylanthracene-1,5-dione (DDTTA) and 7,7,8,8-tetracyanoquinodimethane (TCNQ) results in two new polymorphs of the previously reported charge transfer salt DDTTA(TCNQ)$_2$. The first of these {β-[DDTTA(TCNQ)$_2$]} crystallizes in the space group $P2_1/c$ with cell dimensions $a=15.04(2)$, $b=6.953(7)$, $c=16.22(2)$ Å, $\beta=99.4(1)^\circ$. The structure of the second polymorph {γ-[DDTTA(TCNQ)$_2$]} could not be determined as a result of small crystal size. The new donor, 2,4,4,6,8,8-hexamethyl-2,4a,6,8a-tetraaza-3,4,7,8-tetrahydroanthracene-1,5-dione (HTTA) also forms a charge transfer salt with TCNQ of composition HTTA·TCNQ·CH_3CN. This salt crystallizes in the space group $P2_1/c$ with $a=8.973(1)$, $b=22.907(4)$, $c=14.048(2)$ Å, $\beta=96.69(1)^\circ$. The magnetic susceptibility of the three new materials and the originally reported structure {α-[DDTTA(TCNQ)$_2$]} was recorded as a function of temperature. Ferromagnetic exchange is observed between DDTTA cations in α-[DDTTA(TCNQ)$_2$] as a result of the molecular alignment brought about by hydrogen bonding. Hydrogen bonding between cations is also observed in HTTA·TCNQ·CH_3CN; however, a slightly different orientation results in weak antiferromagnetic exchange between cations. β-[DDTTA(TCNQ)$_2$] and γ-[DDTTA(TCNQ)$_2$] also show overall antiferromagnetic exchange. In the DDTTA salts, the TCNQ anions are arranged in stacks resulting in semiconducting behavior. In the α and β phases these stacks are dimerized whereas the magnetic susceptibility of the γ phase suggests the stack is tetramerized. In HTTA·TCNQ·CH_3CN the TCNQ anions are arranged in discrete dimers.

In the design of materials with predictable electronic properties, one of the more fundamental problems is the anticipation of solid state structure. Electrical and magnetic properties are critically dependent on both intramolecular and intermolecular interaction, and while the former can be controlled by careful design and synthesis, prediction of crystal structures is an art that is still in its infancy. Recent results with amides and complementary amidines have shown that the structure of such systems can be reasonably anticipated as a result of hydrogen bonding;[1] however, the structures of typical electronic and magnetic materials, particularly those of 7,7,8,8-tetracyano-*p*-quinodimethane (TCNQ), are dominated by π stacking interactions. These interactions allow for the maximum overlap between orbitals of neighboring molecules but because of the effect of Peierls distortions and similar one-dimensional electronic effects, solid state structure can be harder to predict. In particular, Visser and co-workers demonstrated that in the morpholinium and thiomorpholinium series of TCNQ salts, though anion stacking was generally observed, small changes in the cation resulted in very large changes in overall packing.[2] Possibly, more strongly interacting cations may exert more control over the lattice structure.

We previously reported that the TCNQ charge transfer salt of 4a,8a-diaza-2,6-dioxa-3,4,7,8-tetrahydro-4,4,8,8-tetramethylanthracene-1,5-dione [DDTTA(TCNQ)$_2$] possessed, in addition to π stacked arrays of $(TCNQ)_2^-$ anions, an unusual hydrogen bonded arrangement of radical cations.[3] In addition, the trifluoroacetate salt of the DDTTA radical cation showed a similar hydrogen bonding motif.[4] Such an interaction between radical cations may prove important in the design and control of packing structures of electronic materials; consequently, we thought it useful to gain a qualitative idea of the strength of this interaction and to determine if it resulted in any novel electronic interactions. We report here magnetic and spectroscopic properties of the previously reported structure of DDTTA(TCNQ)$_2$. We also report the structure, magnetic and spectroscopic properties of two further polymorphs of DDTTA(TCNQ)$_2$ and the TCNQ salt of the related donor 2,4,4,6,8,8-hexamethyl-2,4a,6,8a-tetraaza-3,4,7,8-tetrahydroanthracene-1,5-dione (HTTA).

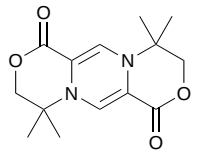

DDTTA

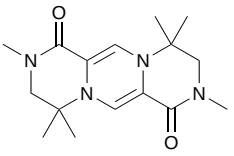

HTTA

Results

As previously reported, combination of DDTTA and TCNQ in hot acetonitrile leads to rapid electron transfer giving paramagnetic solutions containing DDTTA radical cations and TCNQ radical anions. While slow cooling of these solutions gives rise to the triclinic salt previously reported {α-[DDTTA(TCNQ)$_2$]},[3] more rapid cooling leads to the precipitation of two further polymorphs also of composition DDTTA(TCNQ)$_2$. Cooling to room temperature without insulation results in dark green crystals of a monoclinic phase {β-[DDTTA(TCNQ)$_2$]}. If the hot acetonitrile solution is cooled rapidly by immersion in an ice bath, dark green microcrystals of a third phase {γ-[DDTTA(TCNQ)$_2$]} precipitate. HTTA, synthesized in an analogous manner to DDTTA from 3-chloromethyl-1,5,5-trimethylpyrazinone,[5] also reacts with TCNQ in hot acetonitrile giving only one phase, with composition HTTA·TCNQ·CH_3CN. Variation of the crystallization conditions and stoichiometry did not result in other phases.

Single crystal X-ray diffraction on the α phase reveals chains of DDTTA cations, hydrogen bonded in an edgewise arrangement, along with stacks of $(TCNQ)_2^-$ anions (Fig. 1). The O—H distances defining the hydrogen bonds (2.38 Å) are significantly shorter than the sum of the van der Waals radii (2.6 Å). These interactions are not observed in the neutral DDTTA structure. The data show distinct alteration in the TCNQ π stacking distances (a $4\mathbf{k}_f$ or spin Peierls distortion)

† *Present address*: Department of Chemistry, University of Detroit Mercy, 4001 McNichols Rd. Detroit, Michigan, 48219–0900, USA.

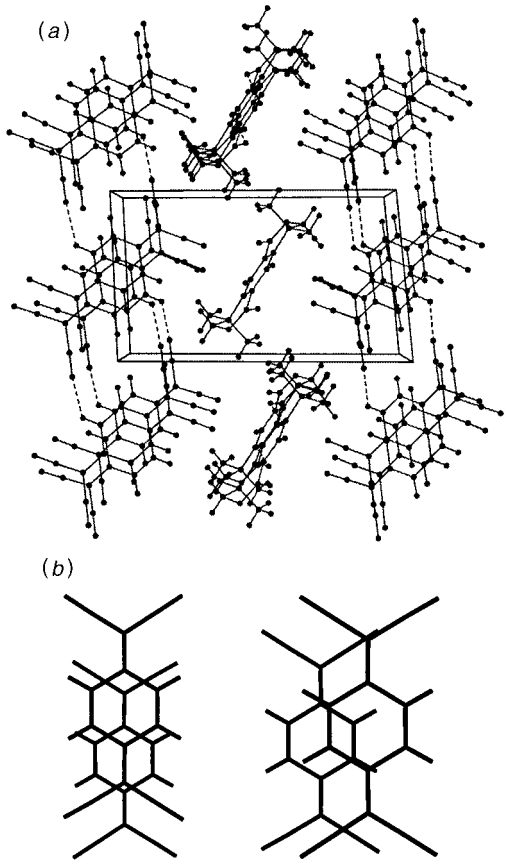

Fig. 1 (*a*) Packing of DDTTA cations and TCNQ anions in α-[DDTTA(TCNQ)$_2$]. The view is down the crystallographic *a* axis. (*b*) Intradimer overlap (left) and interdimer overlap (right) in the TCNQ stack.

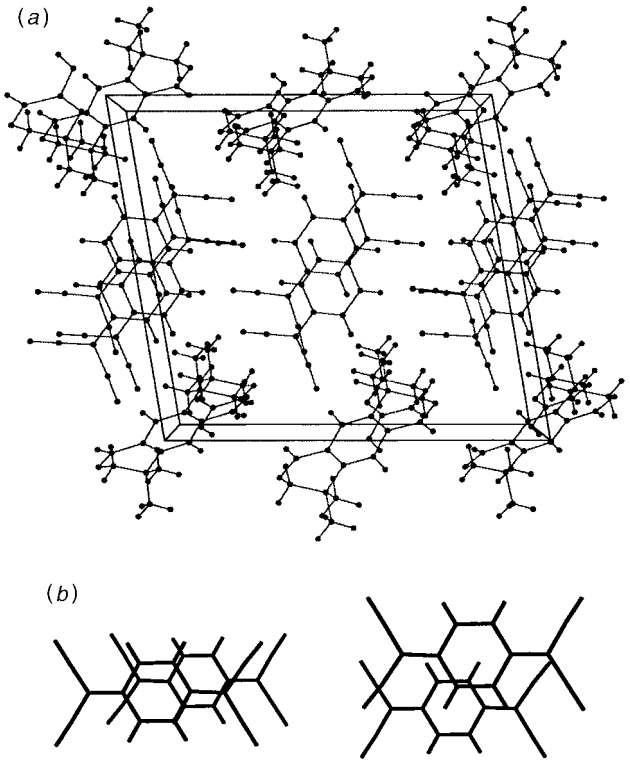

Fig. 2 (*a*) Packing of DDTTA cations and TCNQ anions in β-[DDTTA(TCNQ)$_2$]. The view is down the crystallographic *b* axis. (*b*) Intradimer overlap (left) and interdimer overlap (right) in the TCNQ stack.

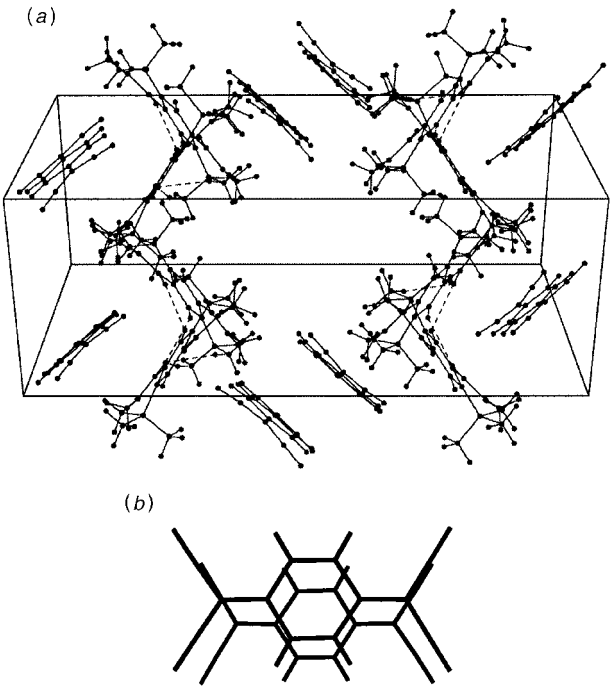

Fig. 3 (*a*) Packing of HTTA cations and $(TCNQ)_2^{2-}$ dimers in HTTA·TCNQ·CH$_3$CN. The acetonitrile solvate has been omitted for clarity. (*b*) Overlap between TCNQ molecules within the dimer.

resulting in the observed semiconducting behavior (*vide infra*).[3] The β phase of DDTTA(TCNQ)$_2$ (Fig. 2) contains herringbone sheets of TCNQ stacks, again showing a $4\mathbf{k}_f$ distortion**.** The DDTTA radical cations are now arranged in 'corrugated sheets' (Fig. 3), separating the anion stacks. Interaction between cations is no longer defined by hydrogen bonding interactions. The HTTA salt shows chains of radical cations similar to those in α-[DDTTA(TCNQ)$_2$], though each cation is tilted with respect to its neighbours by approximately 80° and the C—H···O distance is significantly longer, being very close to the sum of the van der Waals radii (Fig. 2). This appears to be a result of the steric interaction between the amide methyl group and *gem*-dimethyl group of the neighboring cation. The TCNQ anions in this salt are arranged in discrete dimers. The structure of the γ phase could not be determined as a result of extremely small crystal size. Nevertheless, the X-ray powder diffraction pattern indicates that the structure is unique (Table 1). Key intermolecular distances for the determined structures are summarized in Table 2.

Magnetic susceptibility data for the TCNQ salts were recorded as a function of temperature. The data are plotted as χT *vs.* T in Fig. 4. While χT for HTTA·TCNQ·CH$_3$CN and the β and γ phases of DDTTA(TCNQ)$_2$ falls with decreasing temperature, indicating increasing spin pairing or antiferromagnetic behavior, the plot for the α phase passes through a shallow minimum at 75 K. The increase in χT at low temperatures indicates the presence of a ferromagnetic exchange interaction.

Electron paramagnetic resonance (EPR) spectra were recorded on polycrystalline samples of all three phases of DDTTA(TCNQ)$_2$ and HTTA·TCNQ·CH$_3$CN. Spectra were measured over the temperature range 20–300 K. In all cases samples showed single resonances at $g \approx 2.00$ with Lorentzian line shapes and very narrow line widths (<1 G). Signal intensity paralleled magnetic susceptibility. No significant change in line shape or line width was observed as a function of temperature.

While accurate conductivity measurements could not be obtained because of the small crystal size, crude, two-probe conductivity measurements indicate that all three phases of

Table 1 Significant X-ray diffraction lines for the γ phase of DDTTA(TCNQ)$_2$; Cu-Kα radiation, $\lambda = 0.154178$ nm

2θ(°)	d/nm	relative intensity	2θ(°)	d/nm	relative intensity
10.48	0.844	22	21.92	0.405	15
10.92	0.810	43	22.64	0.393	100
11.29	0.784	65	23.21	0.383	15
11.88	0.745	15	24.49	0.363	26
13.49	0.656	22	25.72	0.346	20
14.76	0.600	36	25.95	0.343	15
15.79	0.561	93	27.46	0.325	16
17.48	0.507	18	28.45	0.314	13
18.39	0.482	20	28.78	0.310	17
19.4	0.458	55	30.17	0.296	13
21.6	0.411	11	33.1	0.271	39

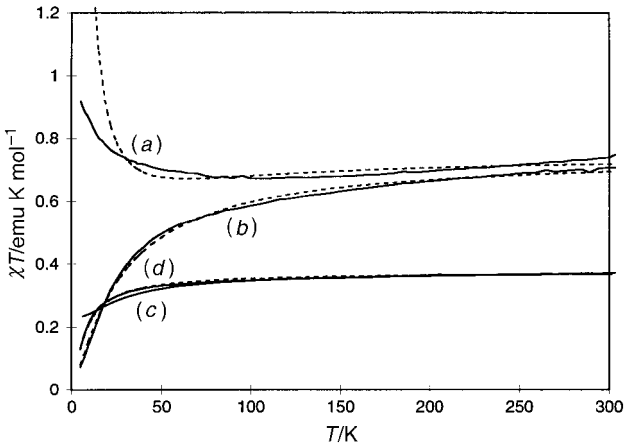

Fig. 4 Plot of the product of molar susceptibility and temperature (χT) *vs.* temperature (solid lines) for (*a*) α-[DDTTA(TCNQ)$_2$], (*b*) β-[DDTTA(TCNQ)$_2$], (*c*) γ-[DDTTA(TCNQ)$_2$], and (*d*) HTTA·TCNQ·CH$_3$CN. The dashed lines are best fits to the models described in the text.

DDTTA(TCNQ)$_2$ are semiconducting with room temperature conductivity $\sigma_{rt} \sim 10^{-3}$ Ω^{-1} cm^{-1} and activation energies of approximately 0.25 eV. Two probe measurements of HTTA·TCNQ·CH$_3$CN indicate that it is an insulator with $\sigma_{rt} \sim 10^{-7}$ Ω^{-1} cm^{-1}.

Optical transmission spectra were measured for the three phases of DDTTA(TCNQ)$_2$ and HTTA·TCNQ·CH$_3$CN. Spectra were recorded over the range 190–25000 nm at 300 K for finely ground samples dispersed in a KBr matrix. All three DDTTA(TCNQ)$_2$ spectra were very similar with broad electronic maxima at 360, 600, 870, 1010 and 3060 nm. The CN stretching vibration was observed at 2202 cm^{-1}. For HTTA·TCNQ·CH$_3$CN the spectrum was significantly different with electronic absorptions at 323, 374, 644 and 877 nm and a TCNQ CN stretch at 2179 cm^{-1}.

Discussion

The CN stretching frequency in TCNQ salts is linearly dependent upon, and can be used to determine, the charge upon each TCNQ molecule.[6] Using this method, the charge per TCNQ for all three DDTTA(TCNQ)$_2$ phases is −0.57. The electronic absorption maxima are consistent with this result and show maxima characteristic of $(TCNQ)_2^{\cdot -}$ dimers.[7] The formula for the DDTTA series of charge transfer salts is thus correctly written DDTTA$^{\cdot +}$(TCNQ)$_2^{\cdot -}$. All three phases show properties typical of salts containing stacked $(TCNQ)_2^{\cdot -}$ anions. Overlap of π orbitals between neighboring TCNQ dimers allows charge transport along the length of the stack. Because of the alternation in spacing of the TCNQ molecules, charge transport is thermally activated and the stacks are semiconducting. The activation energy for conduction (~0.25 eV) is typical for $(TCNQ)_2^{\cdot -}$ stacks.[8,9] This similarity suggests that the DDTTA cations are not significantly involved in charge transport. Magnetic properties of $(TCNQ)_2^{\cdot -}$ stacks are more subtly dependent on packing. Typically they show antiferromagnetic exchange between unpaired electrons and can be modelled as one-dimensional Heisenberg systems with $J/k \approx 50$ K;[9] however, under certain conditions full spin pairing can occur between neighboring $(TCNQ)_2^{\cdot -}$ dimers to form diamagnetic $(TCNQ)_4^{2-}$ tetramers.[8–10] In the case of the DDTTA(TCNQ)$_2$ salts, the magnetic properties are complicated by the presence of magnetic DDTTA$^{\cdot +}$ cations. Plotting the product χT against temperature gives some idea of the overall sign and magnitude of exchange interactions. For non-interacting spins χT is independent of T and the plot is a straight horizontal line. If exchange tends to align the spins antiparallel (antiferromagnetic exchange) the plot curves downwards with decreasing temperature. If exchange tends to align the spins parallel (ferromagnetic exchange) the plot curves upwards with decreasing temperature.[11] For the β phase of DDTTA(TCNQ)$_2$ the plot of χT has a value of 0.72 at room temperature corresponding to two unpaired spins per formula unit. As the temperature is reduced χT drops, indicating overall antiferromagnetic interactions. The plot is reasonably well approximated by two antiferromagnetic Heisenberg one dimensional magnets with $J_1 = -45$ K and $J_2 = -16$ K [Plotted as a dashed curve (*b*) in Fig. 4]. For the γ phase of DDTTA(TCNQ)$_2$ and for HTTA·TCNQ·CH$_3$CN, the room temperature value of χT of 0.37 corresponds to only one unpaired electron per formula unit and the drop in χT indicates weak antiferromagnetic exchange. In the case of the HTTA salt this is readily explained by the discrete $(TCNQ)_2^{2-}$ dimers observed in the crystal structure. Exchange between the two radical anions forming the dimer is strong enough that the dimer is diamagnetic even at room temperature. Similar dimers are observed in the decamethyl ferricenium salt of TCNQ.[12] The observed susceptibility thus results from the HTTA cations alone and can be successfully modelled as a one dimensional Heisenberg magnet with $J = -6$ K [plotted as dashed curve (*c*) in Fig. 4]. Unfortunately the structure of the γ phase could not be determined; however, the magnetic, electronic and optical properties are consistent with the structure containing $(TCNQ)_4^{2-}$ stacks. Strong antiferromagnetic exchange within TCNQ tetramers results in the stack being essentially diamagnetic and the observed susceptibility results from DDTTA cations. Nevertheless, there is significant interaction between tetramers such that charge transport occurs along their length giving rise to the observed conductivity. Tetrameric TCNQ stacks are expected to have very similar optical properties to

Table 2 Selected intermolecular distances for TCNQ salts of DDTTA and HTTA

	α-[DDTTA(TCNQ)$_2$]	β-[DDTTA(TCNQ)$_2$]	HTTA·TCNQ·CH$_3$CN
intradimer TCNQ distance/Å	3.19	3.26	3.14
interdimer TCNQ distance/Å	3.40	3.42	—
intercation CH-O distance/Å	2.38	—	2.52, 2.53

dimer stacks (they are effectively, dimers of dimers).[10] Though additional absorption bands can result from the interaction between dimers, these bands are weak and challenging to detect.[10] Consequently, the optical spectrum of the γ phase does not confirm or disprove the existence of $TCNQ_4^{2-}$ structural units.

The most challenging data to interpret is that for the $DDTTA(TCNQ)_2$ α phase. While the crystal structure, conductivity and optical spectra all indicate the presence of stacks of $(TCNQ)_2^{\cdot -}$ dimers, and χT at room temperature corresponds to two electrons per formula unit, the plot of χT *vs.* T is almost invariant with temperature down to 20 K where it rises slightly as T approaches zero. The simplest possible explanation for such behavior is that the spins interact with each other only very weakly; however, the EPR spectra, conductivity and optical spectra are all inconsistent with this model. The extremely narrow EPR line width and Lorentzian line shape is indicative of exchange narrowing. Exchange interactions allow spin excitations to move rapidly from molecule to molecule within the crystal lattice, such that over the EPR timescale nuclear hyperfine interactions average to zero and a very narrow line is observed. The optical spectrum and the thermally activated conductivity are also inconsistent with weak exchange interactions. As previously mentioned, the optical absorptions result from the charge transfer interaction between TCNQ molecules in the $TCNQ_2^{\cdot -}$ dimer, and the conductivity results from the transfer of unpaired electrons along the TCNQ stack resulting in a net charge transfer (or current) from one end of the stack to the other. Both of these effects result from direct interaction of electrons in neighboring molecules. With such measurable effects of electronic interaction, the assumption that exchange is weak becomes very hard to support.

The next most reasonable model is that there are conflicting exchange interactions that result in little overall susceptibility change with temperature. It is probable that exchange is antiferromagnetic along the TCNQ stacks. If exchange between DDTTA molecules is ferromagnetic, the conflicting interactions may account for the observed behavior. A fit to a model consisting of an antiferromagnetic and a ferromagnetic Heisenberg chain is shown in Fig. 4 [dashed line (*a*)], with $J_{AF}/k = -45$ K and $J_F = 16$ K. Though the fit is reasonable at high temperatures, at low temperatures the model predicts values of χT considerably higher than observed. This may be a result of exchange between DDTTA chains and TCNQ stacks; if the system were truly one dimensional, the EPR line shape would not be Lorentzian.[13] Unfortunately, modelling interchain exchange is a challenging task. While one dimensional systems can be modelled by extrapolating the results from several finite, circular chain models,[14] an analogous treatment for two dimensional systems suffers from the far greater number of spins that must be considered to obtain a series of data from which a useful extrapolation can be made. A confirmation of ferromagnetic exchange between DDTTA cations might be obtained through examination of the trifluoroacetate salt of DDTTA radical cation ($DDTTA{\cdot}CF_3{\cdot}CO_2{\cdot}2CF_3CO_2H$). This salt shows a very similar hydrogen bonding arrangement to α-[$DDTTA(TCNQ)_2$], with the exception that the hydrogen bonds form dimers rather than infinite chains.[4] Unfortunately, determination of the magnetic susceptibility of this salt was severely complicated by loss of solvate and resulting collapse of the crystal structure such that no meaningful data were obtained.

Conclusions

The α phase of $DDTTA(TCNQ)_2$, $HTTA{\cdot}TCNQ{\cdot}CH_3CN$ and DDTTA trifluoroacetate all illustrate that the C—H···O hydrogen bonding between these radical cations is a significant structural motif. The significant differences between magnetic properties of the different phases suggests that relatively well understood intermolecular forces such as hydrogen bonding, may be used to manipulate other intermolecular interactions, such as magnetism, in the solid state. The balance between competing forces can be very delicate as demonstrated by the existence of all three phases of $DDTTA(TCNQ)_2$ at room temperature. The DDTTA cation and its analogues may be useful for forming new magnetic materials; however, in order to obtain greater control of the solid state structure, stable radicals that can form stronger, and more predictable, hydrogen bonds are required. The design and synthesis of such molecules is currently underway in our laboratory.

Experimental

Syntheses of DDTTA and HTTA are described elsewhere. TCNQ was purified by recrystallization from acetonitrile. IR spectra were measured at 300 K on a Perkin Elmer λ-9 grating spectrometer (200–3000 nm) or a Perkin Elmer 1600 series Fourier Transform spectrometer (4000–700 cm^{-1}). Samples were finely powdered and dispersed in potassium bromide. Magnetic susceptibilities were measured on an MPMS SQUID magnetometer and corrected for sample holder diamagnetism. Data were fitted by non-linear least squares regression to the function reported by Smith and Friedberg for a one dimensional Heisenberg magnet.[15] For the α and β phases of $DDTTA(TCNQ)_2$, data were fitted to the sum of two such functions, each with different exchange constants.

Reaction of DDTTA with tetracyanoquinodimethane (TCNQ)

α Phase. Tetracyanoquinodimethane (102 mg, 0.5 mmol) was dissolved in 25 ml of acetonitrile by heating the solution with a hot water bath (60 °C). Under a nitrogen atmosphere, 139 mg of DDTTA was added in one portion. The flask was insulated with glass wool and a Dewar flask containing hot water and allowed to cool to room temp. Long purple–black metallic needles were deposited. X-Ray analysis gave the following cell contents and dimensions: $C_{14}H_{18}N_2O_4{\cdot}2C_{12}H_4N_4$: $M_w = 686.7$; triclinic, $P\bar{1}$ (No. 2); $a = 7.257(1)$, $b = 8.743(2)$, $c = 14.184(2)$ Å, $\alpha = 85.49(1)$, $\beta = 87.06(1)$, $\gamma = 74.59(1)°$; $V = 864.5(3)$ Å^3; $D_c = 1.319$ g cm^{-3}. 1639 reflections were observed with $F > 4.0\,\sigma(F)$. Solution (direct methods) and refinement gave $R = 4.04\%$, $wR = 4.62\%$.

β Phase. Tetracyanoquinodimethane (102 mg, 0.5 mmol) was dissolved in 15 ml of acetonitrile by heating the solution with a hot water bath (60 °C). Under a nitrogen atmosphere, 139 mg of DDTTA was added in one portion and the resulting deep green solution allowed to cool to room temp. Filtration of the resulting suspension gave the TCNQ salt (112 mg) as greenish black needles. This had IR bands (KBr pellet) at 2202 cm^{-1} (CN triple bond stretch) and 1720 cm^{-1} (C=O stretch). Elemental analysis revealed a 1:2 stoichiometry of DDTTA to TCNQ. Calc. for $C_{38}H_{26}N_{10}O_4$: C, 66.47; H, 3.82; N, 20.40. Found: C, 66.54; H, 3.83; N, 20.32%. X-Ray analysis gave the following cell contents and dimensions: $C_{14}H_{18}N_2O_4{\cdot}2C_{12}H_4N_4$: $M_w = 686.7$; monoclinic, $P2_1/c$ (No. 14); $a = 15.04(2)$, $b = 6.953(7)$, $c = 16.22(2)$ Å, $\beta = 99.40(11)$, $V = 1673(4)$ Å^3; $D_c = 1.363$ g cm^{-3}, $D_{obs} = 1.34$ g cm^{-3}. Data collection used the Wyckoff ω scan technique because of the poor crystal quality; 608 reflections were observed with $F > 4\sigma(F)$. Solution (direct methods) and refinement gave $R = 10.52\%$, $wR = 12.27\%$. The high residuals were probably a result of the very small crystal size and poor crystal quality.

γ Phase. Repetition of the procedure for the monoclinic form, with the exception that the solution was cooled rapidly

in an ice bath, led to the precipitation of a green solid. Calc. for $C_{38}H_{26}N_{10}O_4$: C, 66.47; H, 3.82; N, 20.40. Found: C, 64.91; H, 4.27; N,18.60%. The rapid crystallization conditions precluded the formation of high purity crystals. The density was measured by flotation as $D_{obs} = 1.34$ g cm^{-3}. X-Ray powder diffraction data were collected on a sample of the material indicating that it was clearly different from either of the above phases or the starting materials. Unfortunately an indexing scheme consistent with the observed reflections could not be derived.

Reaction of HTTA with TCNQ

TCNQ (102 mg) was dissolved in 20 ml of hot acetonitrile under nitrogen. HTTA (152 mg) was added in one portion and the mixture stirred until solution was complete. The green solution was allowed to cool to room temp. and the purple–black, metallic crystals of the HTTA TCNQ salt removed by filtration (88 mg, 49%): ν_{max}(KBr)/cm^{-1} 1648 (C=O), 2179 (CN); C, 64.96; H, 5.69; N, 22.66; $C_{30}H_{31}N_9O_2$ requires C, 65.57; H, 5.65; N, 22.95%. A large proportion of the crystals formed were twinned which made the collection of X-ray data difficult. However, a crystal was found (dimensions 0.8 x 0.4×0.1 mm) which, though twinned, had sufficiently resolved sets of reflections to allow a unit cell determination and a consistent set of data to be recorded. Data were collected at $-100\,^{\circ}$C in an attempt to reduce the thermal motion of the acetonitrile solvate. This gave the following unit cell parameters; $C_{16}H_{24}N_4O_2 \cdot C_{12}H_4N_4 \cdot CH_3CN$: $M_w = 549.6$; monoclinic, $P2_1/c$ (No. 14); $a = 8.973$ (1), $b = 22.907$ (4), $c = 14.048$ (2) Å; $\beta = 96.69$ (1)°; $V = 2867$ Å^3; $D_c = 1.273$ g cm^{-3}; 2978 reflections were observed with $F > 4\,\sigma(F)$. Solution (direct methods) and refinement gave $R = 6.54\%$, $wR = 8.03\%$.‡

We would like to thank Brenda Conklin and Ron Goldfarb for magnetic susceptibility measurements. This work was funded by grants from the Petroleum Research Fund (31622-AC) and National science foundation (CHE–8903637)

References

1 J. A. Zerkowski, C. T. Seto and G. M. Whitesides, *J. Am. Chem. Soc*., 1992, **114**, 5473.
2 R. J. J. Visser, J. L. De Boer and A. Vos, *Acta Crystallogr. Sect. B*, 1993, **49**, 859.
3 D. J. R. Brook, R. C. Haltiwanger and T. H. Koch, *J. Am. Chem. Soc*., 1991, **113**, 5910.
4 D. J. R. Brook, R. C. Haltiwanger and T. H. Koch, *J. Am. Chem. Soc*., 1992, **114**, 6017.
5 D. J. R. Brook, B. Noll and T. H. Koch, *J. Chem. Soc., Perkin Trans 1*, in the press.
6 J. S. Chappell, A. N. Bloch, W. A. Bryden, M. Maxfield, T. O. Poehler and D. O. Cowan, *J. Am. Chem. Soc*., 1981, **103**, 2442.
7 V. Zelezny, J. Petzelt and R. Swietlik, *Phys. Status Solidi* **B**, 1987, **140**, 595.
8 G. A. Sawatsky, S. Huizinga, J. Kommandeur, K. Kopinga and W. J. M. de Jonge, in *Quasi One-Dimensional Conductors 2*, ed. S. Barisic, A. Bjelis, J. R. Cooper and B. Leontic, Springer Verlag, Berlin, 1979.
9 G. A. Sawatsky, S. Huizinga and J. Kommandeur, in *Quasi One-Dimensional Conductors 2*, ed. S. Barisic, A. Bjelis, J. R. Cooper and B. Leontic, Springer Verlag, Berlin, 1979.
10 K. Yakushi, M. Iguchi, G. Katagiri, T. Kusaka, T. Ohita and H. Kuroda, *Bull. Chem. Soc. Jpn*., 1981, **54**, 348.
11 R. L. Carlin, *Magnetochemistry*, Springer Verlag, Berlin, 1986.
12 D. B. Tanner, J. S. Miller, M. J. Rice and J. J. Ritsko, *Phys. Rev. B*, 1980, **21**, 5835.
13 D. Gatteschi and R. Sessoli, *Magn. Reson. Rev*., 1990, **15**, 1.
14 W. E. Hatfield, *J. Appl. Phys*., 1981, **52**, 1985.
15 T. Smith and J. Friedberg, *Phys. Rev*., 1968, **176**, 660.

Paper 7/04946C; *Received* 10*th July*, 1997

‡ Full crystallographic details, excluding structure factors, have been deposited at the Cambridge Crystallographic Data Centre (CCDC). See Information for Authors, *J. Mater. Chem*., 1997, Issue 1. Any request to the CCDC for this material should quote the full literature citation and the reference number 1145/58.